Correlation effects on the fine-structure splitting within the $3d^9$ ground configuration in highly-charged Co-like ions*

Xue-Ling Guo(郭学玲)[1,2], Min Huang(黄敏)[1,2], Jun Yan(颜君)[3,4], Shuang Li(李双)[1,2], Kai Wang(王凯)[3,4,5], Ran Si(司然)[1,2], and Chong-Yang Chen(陈重阳)[1,2,†]

[1] *Applied Ion Beam Physics Laboratory of Key Laboratory of the Ministry of Education, Fudan University, Shanghai* 200433, *China*
[2] *Shanghai EBIT Lab, Institute of Modern Physics, Department of Nuclear Science and Technology, Fudan University, Shanghai* 200433, *China*
[3] *Institute of Applied Physics and Computational Mathematics, Beijing* 100088, *China*
[4] *Center for Applied Physics and Technology, Peking University, Beijing* 100871, *China*
[5] *Hebei Key Lab of Optic-electronic Information and Materials, the College of Physics Science and Technology, Hebei University, Baoding* 071002, *China*

(Received 24 July 2015; revised manuscript received 31 August 2015; published online 1 December 2015)

A comprehensive theoretical study of correlation effects on the fine-structure splitting within the ground configuration $3d^9$ of the Co-like Hf^{45+}, Ta^{46+}, W^{47+}, and Au^{52+} ions is performed by employing the multi-configuration Dirac–Hartree–Fock method in the active space approximation. It shows that the core-valence correlation with the inner-core 2p electron is more significant than with the outer 3p and 3s electrons, and the correlation with the 2s electron is also noticeable. The core–core correlation seems to be small and can be ignored. The calculated $^2D_{3/2,5/2}$ splitting energies agree with the recent electron-beam ion-trap measurements [*Phys. Rev. A* **83** 032517 (2011), *Eur. Phys. J. D* **66** 286 (2012)] to within the experimental uncertainties.

Keywords: correlation effects, multi-configuration Dirac–Hartree–Fock method, high-Z Co-like ions, fine-structure splitting

PACS: 31.15.ag, 31.15.aj, 31.15.am **DOI:** 10.1088/1674-1056/25/1/013101

1. Introduction

Atomic spectroscopic properties of highly-charged ions (HCIs) are of great importance in atomic physics, astronomical physics, and fusion plasma research.[1–4] Among them the electric-dipole forbidden transition lines are of particular importance in plasma diagnostics due to their sensitive intensities to electron temperature and density and other plasma parameters.[5–11] The currently famous elements (for example, tungsten and gold) have inspired great research interest since their favorable physical properties, and many spectra lines have been measured with high accuracy.[12–22] Meanwhile, the accurately measured properties, such as wavelength, can provide crucial tests for atomic structure theory of both the electron correlation and relativistic corrections,[23,24] which are the major questions in theoretical calculations.

Ralchenko *et al.*[24] and Osin *et al.*[25] measured many forbidden lines from the HCIs of hafnium (Hf, $Z = 72$), tantalum (Ta, $Z = 73$), tungsten (W, $Z = 74$), and gold (Au, $Z = 79$) with an open 3d shell, with a wavelength uncertainty of 0.03%. Unfortunately, the calculated wavelengths, obtained by Ralchenko and Osin *et al.*[24,25] using the relativistic configuration-interaction (RCI) method implemented in the flexible atomic code (FAC),[26,27] can only agree with the experimental ones in 0.8%. Quinet[28] later obtained the energy levels, wavelengths, and transition probabilities for tungsten ions between W^{47+} and W^{61+} by using the fully relativistic multi-configuration Dirac–Fock (MCDF) method with the latest version of GRASP, i.e., the general purpose relativistic atomic structure package by Norrington *et al.*[29] However, due to the limited configuration interaction considered, the calculated wavelengths differ from the measured ones by up to 0.7%. Fournier[30] also performed calculations for W^{47+} by using the fully relativistic parametric potential code (RELAC),[31] but the quantum electrodynamic (QED) corrections were not included.[32] It is obvious that the differences between these calculated wavelengths and measured ones are much larger than the stated experimental uncertainties, which may mean that there is a long way to go on the theoretical side.

Recently, by means of the second-order relativistic many-body perturbation theory (RMBPT) approach, we have updated the energy levels and the transition data for these forbidden transitions among the levels within the ground configurations [Ar] $3d^k (k = 1, ..., 9)$ in Co-like through K-like ions of Hf, Ta, W, and Au elements.[33] This RMBPT approach is based on the work of Lindgren on Rayleigh–Schrödinger perturbation theory extended to a multi-configurational zero-

*Project supported by the National Natural Science Foundation of China (Grant Nos. 11076009 and 11374062), the Chinese Association of Atomic and Molecular Data, the Chinese National Fusion Project for ITER (Grant No. 2015GB117000), and the Leading Academic Discipline Project of Shanghai City, China (Grant No. B107).

†Corresponding author. E-mail: chychen@fudan.edu.cn

© 2016 Chinese Physical Society and IOP Publishing Ltd

order wave function,[34] which is also implemented in the FAC code.[26,27] The RMBPT calculation dramatically removes the existing systematic deviations for wavelengths in previous theoretical calculations and reproduces these measured wavelengths to within 0.2%, which greatly improves the existing theoretical accuracy mentioned above, though still fall outside the experimental uncertainties, 0.03%, remotely.

To date, another state-of-the-art method with high accuracy is the multi-configuration Dirac–Hartree–Fock (MCDHF) approach implemented in the GRASP2K-V3 package,[35] which is a revised version of GRASP2K by Jönsson *et al.*[37] This approach is suitable to study different physical effects step by step.[37] In this work, with the purpose of analyzing the correlation effects clearly and getting the calculated transition energies close to the experimental data, by means of the MCDHF approach, we focus on the forbidden transition within the relatively simple multi-valence cobalt-like ions, which have the ground configuration $3d^9$, with nine valence electrons, i.e., one-vacancy-electron outside the closed core subshell. The one-vacancy-electron system is similar to the one-valence-electron system,[38,39] but should involve more complex correlations.

Furthermore, to investigate the core–valence (CV) correlation effects clearly, two independent approaches, the separate core–valence approach (SCV) and the full core–valence approach (FCV), are adopted. By comparison and analysis, we prove that the SCV is beneficial to give reliable information about important correlation contribution from separate subshell quickly. It is found that the electron correlation from the inner core 2p makes significant contribution to the transition energy, even larger than from the outer electron 3p. At the same time, the contribution from deeper core electron 2s is larger than from the 3s, which also should be considered. The final calculated fine-structure separation are in excellent agreement with the experimental results to within 0.01%.

2. Theoretical approach

In the MCDHF method, the ion is represented by the atomic state functions (ASF) $\Psi(\gamma J)$, which is a linear combination of a number of configuration state functions (CSF)

$$\Psi(\gamma J) = \sum_i c_i \Phi(\gamma_i J), \tag{1}$$

where the CSFs $\Phi(\gamma_i J)$ are constructed from single-electron Dirac orbitals, which are based on the well-known rules of symmetry (parity and angular momenta).[40] The coefficients c_i and the radial parts in the CSFs are determined by solving the MCDHF equations which are derived by using the variational approach, within the relativistic self-consistent field (RSCF) method.[41] The radial functions are numerically represented on a logarithmic grid and are orthogonalized by introducing the Lagrange multipliers.[41,42] In the variational part of the calculations, we include the Dirac–Coulomb (DC) Hamiltonian (in a.u.), which can be written as

$$H_{\rm DC} = \sum_{i=1}^{N} [c\alpha_i p_i + (\beta_i - 1)c^2 + V(i)] + \sum_{i<j}^{N} \frac{1}{r_{ij}}. \tag{2}$$

Once we obtain a set of radial orbitals, relativistic configuration interaction calculations (RCI)[43] can be performed. In the RCI calculations we include the transverse photon interaction in the Hamiltonian[44]

$$H_{\rm trans} = -\sum_{i<j}^{N} \left[\alpha_i \alpha_j \frac{\cos(\omega_{ij} r_{ij}/c)}{r_{ij}} + (\alpha_i \cdot \nabla_i)(\alpha_j \cdot \nabla_j) \frac{\cos(\omega_{ij} r_{ij}/c) - 1}{\omega^2 r_{ij}/c^2} \right]. \tag{3}$$

The photon frequency ω_{ij} used by the RCI program in calculating the matrix elements of the transverse photon interaction is taken to be the difference in the diagonal Lagrange multipliers and associated with orbitals. When using the low frequency limit $\omega_{ij} \to 0$, the interaction is usually referred to as the Breit interaction. The calculation of the quantum electrodynamic corrections (QED) due to the other leading part of self-energy (SE) and vacuum polarization (VP) are also included in the RCI calculation.[45]

One main advantage of the multiconfigurational method is the fact that correlation can be included in a systematic way, by using the notion of an active set (AS) of orbitals, that are in turn used to generate CSFs.[46] The foundation of this approach is a restricted active space (RAS) method,[47] where the active set of orbits is systematically increased. Considering the relative importance of different excitations from the view point of order-by-order expansion of energy in perturbation theory, we allow single (S) and double (D) replacement from the reference configurations to an active set. According to this approach, the atomic electrons are divided into two types: valence electrons and core electrons. The correlations are then classified into three types, i.e., the valence–valence (VV), core–valence (CV), and core–core (CC) correlations. It should be mentioned that the CC correlation can be further classified according to (a) intra-CC, i.e., correlation within one core subshell; and (b) inter-CC, i.e., correlation between two core subshells. The details of this approach can be found elsewhere.[37,48]

3. Calculation procedure

3.1. DHF calculation

At first, the DHF calculation is performed for the single $3d^9$ configuration. After a set of radial orbitals have been obtained, the RCI calculations can been done, by which the relativistic corrections are included. Table 1 shows the specific contributions to the transition energy ($\Delta E = E(^2D_{3/2}) - E(^2D_{5/2})$) between the fine-structure levels of $3d^9$ $^2D_{3/2}$ and

$^2D_{5/2}$ from the DHF calculation. As expected, the DC contribution is the dominating part, and the Breit interaction giving a significant correction, decreasing the fine-structure splitting by about 2%. Among the QED effects, the SE is more important and increased by about 0.17%, whereas the VP could almost be ignored. In the following calculations, all results are obtained from the RCI calculations.

Table 1. Relativistic and QED effects on the fine-structure splitting (ΔE) (in cm^{-1}) between the $3d^9\ ^2D_{3/2}$ and $^2D_{5/2}$ levels from the DHF calculations.

Ion		ΔE_{DC}	δE_{Breit}	δE_{QED}		ΔE_{DHF}
				δE_{SE}	δE_{VP}	
$Z=72$	Hf^{45+}	479319	−10160	830	0	469989
$Z=73$	Ta^{46+}	512716	−10730	889	1	502876
$Z=74$	W^{47+}	547862	−11324	952	1	537490
$Z=79$	Au^{52+}	751661	−14657	1315	1	738320

3.2. VV correlation calculation

On the base of the DHF calculation, the contributions of the different correlations are obtained by way of increasing the active sets (AS) layer by layer. In this VV model, we set the Ar-like $1s^22s^2\cdots3p^6$ core inactive and only allow the outside 3d valence electron to be excited to the AS by SD replacement. Then, the AS is increased as follows:

$$\mathrm{AS}_1 = 3\mathrm{d} + \{4\mathrm{s}, 4\mathrm{p}, 4\mathrm{d}, 4\mathrm{f}\},$$

$$\mathrm{AS}_2 = \mathrm{AS}_1 + \{5\mathrm{s}, 5\mathrm{p}, 5\mathrm{d}, 5\mathrm{f}, 5\mathrm{g}\},$$

$$\mathrm{AS}_3 = \mathrm{AS}_2 + \{6\mathrm{s}, 6\mathrm{p}, 6\mathrm{d}, 6\mathrm{f}, 6\mathrm{g}\},$$

$$\mathrm{AS}_4 = \mathrm{AS}_3 + \{7\mathrm{s}, 7\mathrm{p}, 7\mathrm{d}, 7\mathrm{f}, 7\mathrm{g}\}.$$

We note that the main VV contribution comes from $n=4$ complex, and the contributions from $n=7$ and 8 vary very little. The effects of high-l (h and i) orbitals on the fine-structure splitting have also been tested and found to be negligible (6 to 10 cm^{-1}). Hence we conclude that the AS_4 mentioned above is enough to reach convergence (see Fig. 2). The splitting energies for the four ions of Hf^{45+}, Ta^{46+}, W^{47+}, and Au^{52+} from the VV model, that is ΔE_{VV}, are given in Table 2, and also in Tables 3 and 5 for further comparison.

3.3. CV correlation calculation

In the subsequent calculations, the CV correlation is successively included. We applied two strategies in this work to explore the importance of CV correlations, i.e., separate core valence (SCV) (see Section 3.3.1) and full core valence (FCV) (see Section 3.3.2). The SCV method can be used to probe the influence of one subshell at the time, on the fine-structure of the ground term. The FCV method is the final large-scale CV calculation by including full-core-valence correlation by SD excitation from all the involved core subshells simultaneously, which can be used to check the degree of approximation of SCV and the accuracy of the whole calculations.

Table 2. The fine-structure splitting ($\Delta E_{SCV}(nl)$) and the net core–valence contributions ($\delta E_{SCV}(nl)$, see text) from each core orbital (nl) from the SCV model for the Hf^{45+}, Ta^{46+}, W^{47+}, Au^{52+} ions along with AS_n. The ΔE_{VV} from VV model given for comparisons. The total CV contributions from SCV are also given. Values are given in cm^{-1}.

AS	ΔE_{VV}	SCV										
		$\Delta E_{SCV}(nl)$					$\delta E_{SCV}(nl)$					
		3p	3s	2p	2s	1s	3p	3s	2p	2s	1s	sum
						Hf^{45+}						
AS_1	470339	469912	470388	470940	470380	470341	−428	48	601	41	1	263
AS_2	470356	470022	470401	471130	470436	470360	−334	46	774	81	5	572
AS_3	470372	470053	470423	471183	470467	470383	−319	51	811	95	11	649
AS_4	470373	470063	470426	471200	470473	470389	−310	52	827	100	16	685
						Ta^{46+}						
AS_1	503246	502811	503297	503871	503288	503247	−435	51	625	43	1	286
AS_2	503263	502925	503311	504067	503347	503268	−338	49	805	84	5	605
AS_3	503280	502958	503334	504122	503379	503291	−322	54	842	99	12	685
AS_4	503281	502968	503337	504140	503385	503298	−313	56	859	104	17	723
						W^{47+}						
AS_1	537876	537430	537931	538524	537921	537878	−447	54	648	44	1	300
AS_2	537894	537544	537943	538734	537982	537899	−350	50	840	88	5	633
AS_3	537912	537577	537968	538786	538014	537924	−335	56	874	103	12	710
AS_4	537913	537590	537971	538803	538019	537930	−322	58	890	106	17	750
						Au^{52+}						
AS_1	738832	738368	738905	739614	738886	738833	−464	74	782	55	2	449
AS_2	738853	738505	738924	739856	738959	738859	−348	71	1003	106	6	838
AS_3	738876	738549	738953	739924	739001	738890	−326	77	1048	125	14	939
AS_4	738877	738561	738957	739946	739008	738898	−316	80	1069	131	21	985

Table 3. The fine-structure splitting ($\Delta E_{\rm FCV}(nl)$) and the net core–valence contributions ($\delta E_{\rm FCV}(nl)$, see text) from each core orbital (nl) from the FCV model for the Hf^{45+}, Ta^{46+}, W^{47+}, Au^{52+} ions along with AS_n. The $\Delta E_{\rm VV}$ obtained from VV model is given for comparison. The total CV contributions of FCV are also listed. Values are given in cm^{-1}.

AS	$\Delta E_{\rm VV}$	FCV										
		$\Delta E_{\rm FCV}$					$\delta E_{\rm FCV}(nl)$					
		3p	3s	2p	2s	1s	3p	3s	2p	2s	1s	sum
						Hf^{45+}						
AS_1	470339	469917	469967	470547	470593	470595	−423	50	580	46	2	256
AS_2	470356	470025	470078	470811	470889	470889	−330	52	734	78	0	534
AS_3	470372	470057	470113	470915	471008	471019	−315	56	802	93	12	647
AS_4	470373	470066	470124	470946	471044	471059	−307	58	822	98	15	686
						Ta^{46+}						
AS_1	503246	502816	502869	503473	503521	503523	−430	53	604	48	2	278
AS_2	503263	502929	502984	503747	503828	503828	−334	55	763	81	0	565
AS_3	503280	502961	503021	503854	503951	503963	−318	60	833	97	12	683
AS_4	503281	502971	503032	503886	503988	504003	−310	61	854	102	16	723
						W^{47+}						
AS_1	537876	537430	537486	538114	538164	538166	−447	56	628	50	2	290
AS_2	537894	537546	537604	538397	538481	538481	−348	58	792	84	0	587
AS_3	537912	537580	537643	538508	538609	538621	−332	63	865	101	13	710
AS_4	537913	537590	537655	538541	538647	538663	−323	64	886	106	16	750
						Au^{52+}						
AS_1	738832	738373	738447	739205	739267	739270	−458	74	758	62	3	438
AS_2	738853	738509	738586	739537	739640	739640	−344	77	952	102	0	786
AS_3	738876	738553	738636	739672	739793	739808	−322	83	1036	121	15	932
AS_4	738877	738565	738649	739709	739838	739857	−312	84	1060	129	20	980

Table 4. The fine-structure splitting ($\Delta E_{\rm SCC}(nl)$) and the net core–core correlations ($\delta E_{\rm SCC}(nl)$, see text) from each core orbital (nl) from the SCC model for the Hf^{45+}, Ta^{46+}, W^{47+}, Au^{52+} ions along with AS_n. The total CC contributions from SCC are also given. Values are given in cm^{-1}.

AS	SCC										
	$\Delta E_{\rm SCC}(nl)$					$\delta E_{\rm SCC}(nl)$					
	$3p$	$3s$	$2p$	$2s$	$1s$	$3p$	$3s$	$2p$	$2s$	$1s$	sum
					Hf^{45+}						
AS_1	469918	470384	470981	470384	470345	6	-4	41	4	5	52
AS_2	469981	470399	471147	470438	470359	-40	-2	17	2	-1	-24
AS_3	470013	470420	471196	470467	470385	-40	-2	14	0	2	-26
AS_4	470022	470423	471218	470472	470399	-41	-2	18	-1	9	-16
					Ta^{46+}						
AS_1	502817	503293	503913	503292	503252	6	-4	43	4	5	54
AS_2	502883	503309	504085	503349	503266	-42	-2	17	2	-1	-26
AS_3	502916	503332	504136	503379	503294	-41	-2	14	0	2	-28
AS_4	502925	503335	504159	503384	503308	-42	-2	19	-1	11	-17
					W^{47+}						
AS_1	537436	537926	538570	537925	537883	7	-4	46	4	5	57
AS_2	537502	537943	538745	537984	537898	-42	0	11	2	-1	-30
AS_3	537537	537966	538799	538015	537926	-40	-2	13	1	2	-26
AS_4	537546	537969	538822	538020	537942	-44	-2	18	1	12	-15
					Au^{52+}						
AS_1	738375	738901	739663	738892	738839	7	-5	49	6	6	63
AS_2	738452	738922	739875	738962	738859	-53	-2	19	3	-1	-34
AS_3	738496	738951	739940	739001	738893	-53	-3	16	0	3	-36
AS_4	738506	738954	739968	739008	738918	-55	-3	22	-1	20	-17

Table 5. The fine-structure splitting (ΔE, in cm^{-1}) calculated from the present DHF, VV, SCV, FCV, FCV+SCC model, compared with the other available theoretical results[24,25,28,33] and experimental data with error bars for Hf^{45+}, Ta^{46+}, W^{47+}, Au^{52+} ions.

Ion	$\Delta E^{\rm a}_{\rm DHF}$	$\Delta E^{\rm a}_{\rm VV}$	$\Delta E^{\rm a}_{\rm SCV}$	$\Delta E^{\rm a}_{\rm FCV}$	$\Delta E^{\rm a}_{\rm FCV+SCC}$	$\Delta E_{\rm RCI}$	$\Delta E^{\rm d}_{\rm MCDF}$	$\Delta E^{\rm e}_{\rm RMBPT}$	$\Delta E_{\rm Exp}$
Hf^{45+}	469989	470373	471058	471059	471043	469096[b]		470552	471054 ± 67[b]
Ta^{46+}	502876	503281	504004	504003	503986	548336[b]		503461	503956 ± 76[b]
W^{47+}	537490	537913	538662	538663	538648	536481[c]	535590	538080	538590 ± 87[c]
Au^{52+}	738320	738877	739874	739857	739840	737039[b]		739023	739809 ± 164[b]

[a] Present results; [b] Ref. [25]; [c] Ref. [24]; [d] Ref. [28]; [e] Ref. [33].

3.3.1. Separate core–valence correlation

The separate approach for the CV correlation (SCV) was first proposed for studying Ag-like W^{27+} ion by Fei.[37] In this method, the effect on the fine structure splitting is investigated by including correlation with one core subshell at a time. For example, CV with a 2p electron is included via the CSFs of the form $1s^22s^22p^63s^23p^63d^7nln'l'$ and $1s^22s^22p^53s^23p^63d^8nln'l'$ (this model also includes VV correlation), and the nl and $n'l'$ belong to the AS mentioned above (see Section 3.2).

In Table 2, we present the fine-structure splitting ($\Delta E_{\rm SCV}(nl)$) for each subshell (nl) from the SCV model for the four target ions, along with the net CV contributions $\delta E_{\rm SCV}(nl)(\delta E_{\rm SCV}(nl) = \Delta E_{\rm SCV}(nl) - \Delta E_{\rm VV})$. To clearly show the convergence behavior for the CV correlation as a function of the AS, we plot the $\delta E_{\rm SCV}(nl)$ in Fig. 1. It is clear that $\delta E_{\rm SCV}(nl)$ converges as the active set increases. It shows that except for the outer-core-3p correlation, all the others increase the fine-structure energy separations. The contributions from deep-core 2p are larger than from the outer-core 3p (by a factor of 2–3), while the contributions from deeper-core 2s are larger than from 3s (by 2 times). The CV correlations with the p subshells are considerably larger than with the s subshells. Hence, it is important to include core correlation down to the $n = 2$ shells to account for all important correlation effects.

The sum of all $\delta E_{\rm SCV}(nl)$ is the total CV correlation contributions resulting from the SCV model, which are also given in Table 2 and plotted in Fig. 1. It shows that good convergence is obtained using the CSFs-AS_4 expansion, with difference between the AS_3 and AS_4 splitting being only about 40 cm^{-1} (0.008%). The sum of the net CV contribution and the corresponding $\Delta E_{\rm VV}$, both obtained in the AS_4 calculations, referred to as $\Delta E_{\rm SCV}$, can be used as a preliminary estimation on the fine-structure splitting from the SCV model, which are also given in Table 5.

It is worth noting that, this surprising result also occurs in Ag-like tungsten ion,[37] where correlation effects from deep core 3d is larger than the outer valence electron 4d. Similarly, the 3d gives a positive contribution, but 4d presents a negative effect to the fine structure between the ground state $4d^{10}4f\ ^2F_{5/2}$ and $^2F_{7/2}$. The reason behind this is worth further study.

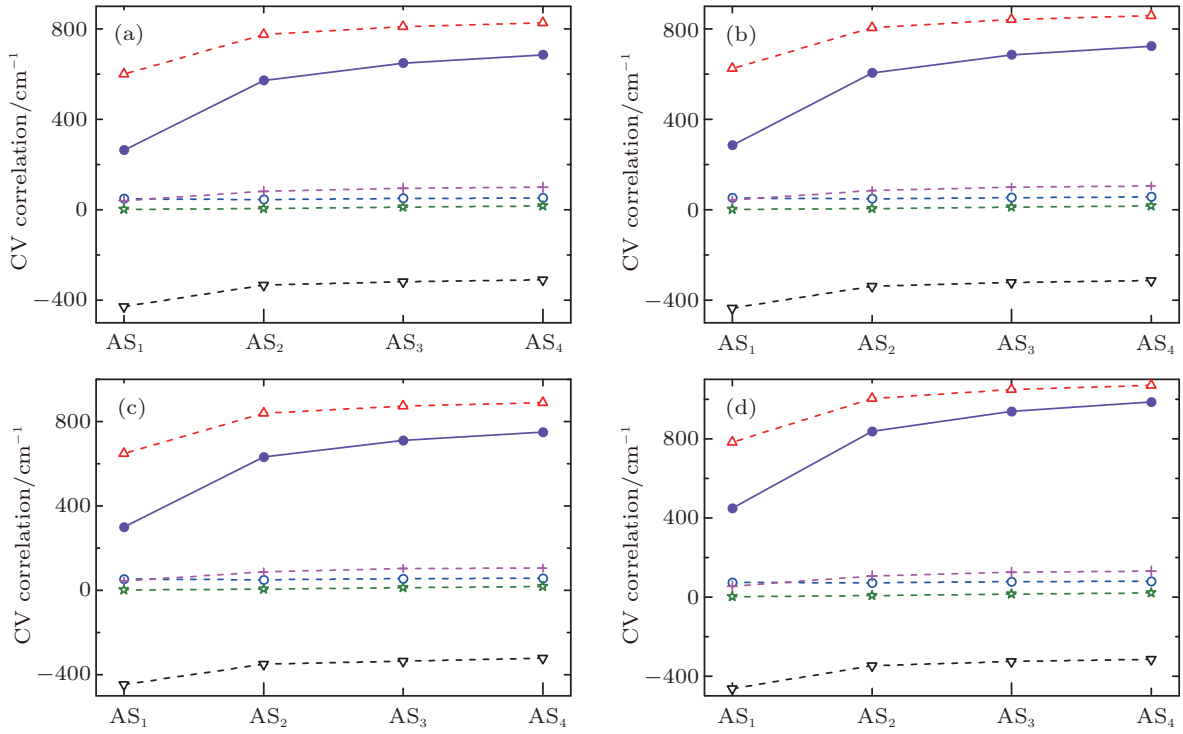


Fig. 1. (color online) Convergence plot for each core (3p, 3s, 2p, 2s, 1s) CV correlation and the total CV correlation to the transition energy for the four (a) Hf^{45+}, (b) Ta^{46+}, (c) W^{47+}, (d) Au^{52+} ions in the SCV model. The dashed lines with down triangles (▽), circles (○), up triangles (△), crosses (+) and stars (⋆) represent the correlation from 3p, 3s, 2p, 2s, 1s in order, while the solid line with dots (•) are the sum of these CV correlation from the SCV model.

3.3.2. Full core–valence correlation

The second approach for the CV correlation study is the full core–valence (FCV) approach, that means correlations would be included in one step for all the involved core electrons, simultaneously. However, for comparison with the SCV model and to see the detailed correlation effects from different core electrons, we include the core electron one-by-one in the order from the outer to inner subshell (i.e., 3p→3s→2p→2s→1s). In practical terms, the core-electron 3p first interacts with valence electrons of active sets, then the inner core electrons of 3s, 2p, 2s, 1s are gradually added one-by-one. Hence, once the innermost core 1s is considered, the

total CV correlation effect is obtained. Here the number of CSFs reaches 238277, which is much larger than the number from SCV for 1s (53731).

Similar to the results listed in Table 2 from the SCV model, the transition energies from the FCV approach ($\Delta E_{\rm FCV}$) are also presented in Table 3, together given are also the net CV contributions $\delta E_{\rm FCV}(nl)$ from each core-subshell. Obviously, due to different calculation procedures from the SCV, there is a difference in the way in which we obtain the $\delta E_{\rm FCV}(nl)$, that is, the net CV effect from 3p is the energy difference relative to the VV model, i.e., $\delta E_{\rm FCV}(3{\rm p}) = \Delta E_{\rm FCV}(3{\rm p}) - \Delta E_{\rm VV}$, while the 3s CV contribution is relative to $\Delta E_{\rm FCV}(3{\rm p})$ ($\delta E_{\rm FCV}(3{\rm s}) = \Delta E_{\rm FCV}(3{\rm s}) - \Delta E_{\rm FCV}(3{\rm p})$), and so on.

By comparing with Tables 2 and 3, we can obtain similar conclusions for the correlation effects on the splitting from the FCV approach as well as from SCV model. The CV contributions from each core orbital calculated in the FCV model are in excellent agreement with the SCV ones. Therefore, to make an exploratory investigation of core–valence effects quickly, the SCV calculation is a good estimate, while to show all CV correlation results at one time, the FCV is a good choice.

3.4. CC correlation calculation

In this step, the CC correlation could be taken into account by applying a similar approach to that for the SCV and FCV, which are referred to as the SCC and FCC model. However, when including all the core–core correlation, the size of the CSF expansions increases rapidly with the AS, and therefore convergence is hard to achieve.

Here we only investigate the intra-CC effects[37] in the SCC model, and the resulting CC correlation contributions ($\Delta E_{\rm SCC}(nl)$) are presented in Table 4. The net CC contribution ($\delta E_{\rm SCC}(nl)$) from each core subshell nl is the corresponding differences between $\Delta E_{\rm SCC}(nl)$ and $\Delta E_{\rm SCV}(nl)$, which are also given in Table 4. From Table 4, it is easy to see that the largest contribution due to the CC correlation is from the 3p orbital and the second one is from 2p, though the contributions from both of them are tiny. The sum of all the net CC correlation only decreases the transition energies around 15 cm^{-1} (by 30 per million) for the four ions. These net CC values are added to the results from FCV calculations, the resulting energies referred to as $\Delta E_{\rm FCV+SCC}$ and given in Table 5, could be regarded as the most accurate fine-structure splitting in the present work, as all kinds of electron correlation have been taken into account.

3.5. Results and discussion

Convergence is one of the most important factors to state the accuracy of theoretical results. Figure 1 shows the convergence of the results calculated in the SCV model. We also display the convergence behavior of energy differences ($\Delta E_{\rm Theo} - \Delta E_{\rm Expt}$) as a function of AS$_n$ for the four ions from the *ab inito* results of the VV and FCV model (see Fig. 2). It

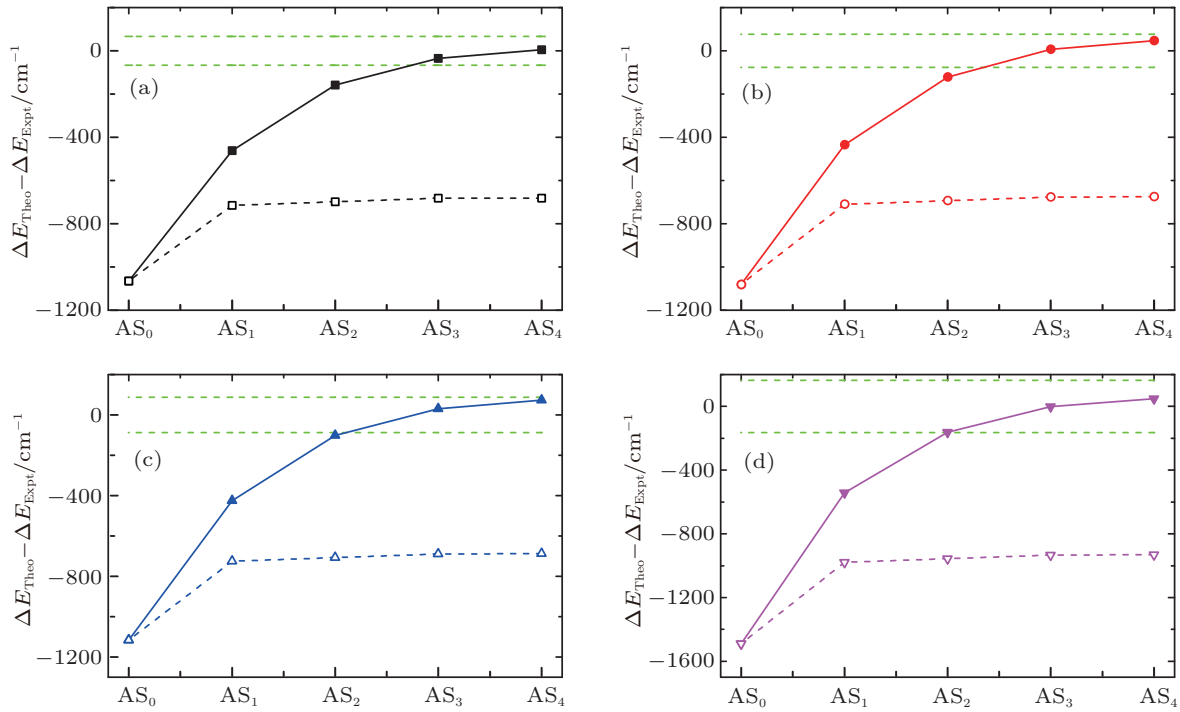


Fig. 2. (color online) Convergence plot of the different approaches (FCV and VV) of the fine-structure splitting compared to the experimental data for (a) Hf^{45+}, (b) Ta^{46+}, (c) W^{47+}, and (d) Au^{52+} ion. The solid lines and the dashed lines respectively represent the differences of FCV and VV from experimental data. The horizontal dashed lines stand for the experimental errors.

shows that the VV model is much easier to reach convergency than the FCV model. That is, the VV model converges when the AS grows to AS_2, while the results converge in AS_4 for the FCV model. It is clear that the CV correlations are critical, increasing significantly the splitting and bringing the calculated results within the experimental uncertainties.

In Table 5, we collect our fine-structure splitting energies obtained from the above-mentioned DHF, VV, SCV, FCV, and FCV+SCC calculations, together with previously published theoretical and experimental data.[24,25,28,33] The splitting energies of VV, SCV, FCV, and FCV+SCC are all calculated using the AS_4-CSFs expansion. The $\Delta E_{\rm VV}$ added by the total CV contribution from each subshell in the SCV model is the $\Delta E_{\rm SCV}$, and the $\Delta E_{\rm FCV}$ is just the $\Delta E_{\rm FCV}(1s)$. The final FCV+SCC results are obtained by adding the total CC correlation contributions from the SCC model to $\Delta E_{\rm FCV}(1s)$, as mentioned above.

By analyzing Table 5, we can see, firstly, the VV-correlation contributions ($\Delta E_{\rm VV} - \Delta E_{\rm DHF}$) are about 384 $\rm cm^{-1}$ and 557 $\rm cm^{-1}$, while the CV-correlation contributions ($\Delta E_{\rm SCV} - \Delta E_{\rm VV}$) are between 685 $\rm cm^{-1}$ and 985 $\rm cm^{-1}$ for the four $Z = 72, 73, 74, 79$ ions. Thus, based on the isoelectronic sequence law, we may conclude that the CV correlations are larger than the VV ones for these Co-like high-Z ($70 < Z < 80$) ions. Secondly, the results from SCV, FCV, and FCV+SCC agree with each other very well, and all of them agree with the measured ones to within the experimental uncertainty (0.03%), which are much better than the previous RCI,[24,25] (up to 0.4%) RMBPT (within 0.1%)[33] using the FAC code,[26,27] and MCDF results (0.6%).[28] It also implies that the CC correlations are small and could be discarded.

4. Conclusions

With the revised GRASP2K-V3 code, we have made a detailed treatment of the electron correlation for the multi-valence-electron systems of Co-like ($3d^9$) ions using the MCDHF approach. Highly accurate fine-structure energies between $^2D_{3/2}$ and $^2D_{5/2}$ are obtained for Hf^{45+}, Ta^{46+}, W^{47+}, and Au^{52+}, being within the experimental uncertainties.[24,25] It shows that it is critical to include the deep core-valence correlation down to the $n = 2$ subshell, to achieve spectroscopic accuracy. In particular, the CV correlation from the deep core 2p is larger than 3p, 2s is larger than 3s, and CV from 1s could be ignored. The CC correction is so small that it could be ignored in the latter large-scale calculations especially for other higher-Z Co-like ions.

Among the SCV and FCV methods used to study CV correlation, the SCV method is reliable enough to get similar accurate results to the FCV model, but with much smaller amount of CSFs and less computation efforts. The SCV method provides a simple and wise way to investigate the core–valence correlation from the individual subshell. The strategies applied here have been successfully employed to investigate the fine-structure splitting within the ground state along with the whole Co I isoelectronic sequence, as well as for the other one-valence sequence (K I and Rb I) and one-vacancy sequence (Rh I). These results are being prepared to be published elsewhere. We believe that the present strategies can also be potentially useful in even more complicated sequences, such as the $nd^k (k = 2, ..., 8)$ ones.

References

[1] Lundqvist M, Nilsson H, Wahlgren G M, Lundberg H, Xu H L, Jang Z K and Leckrone D S 2006 *Astron. Astrophys.* **450** 407
[2] Fischer U, Pereslavtsev P, Möslang A and Rieth M 2009 *J. Nucl. Mater* **386** 789
[3] Seely J F, Ekberg J O, Brown C M, Feldman U, Behring W E, Reader J and Richardson M C 1986 *Phys. Rev. Lett.* **57** 2924
[4] Li B, Higashiguchi T, Otsuka T, Yugami N, Dunne P, Kilbane D, Sokell E and O'ullivan G 2014 *J. Phys. B: At., Mol. Opt. Phys.* **47** 075001
[5] Fan J Z, Zhang D H, Chang Z W, Shi Y L and Dong C Z 2012 *Chin. Phys. Lett* **29** 073102
[6] Eidelsberg M, Crifo-Magnant F and Zeippen C J 1981 *Astro. Astrophys. Suppl. Ser.* **43** 455
[7] Edlén B 1984 *Phys. Scr.* **5** 11
[8] Kaufman V and Sugar J 1986 *J. Phys. Chem. Ref. Data* **15** 321
[9] Biémont E and Zeippen C J 1996 *Phys. Scr.* **1996** 192
[10] Feldman U, Seely J, Landi E and Ralchenko Y 2008 *Nucl. Fusion* **48** 045004
[11] Fan J Z, Wang Q M, Chang Z W and Dong C Z 2012 *Chin. Phys. B* **21** 063102
[12] Brown G V, Hansen S B, Träbert E, Beiersdorfer P, Widmann K, Chen H, Chung H K, Clementson J H T, Gu M F and Thorn D B 2008 *Phys. Rev. E* **77** 066406
[13] Ralchenko Y, Draganic I N, Tan J N, Gillaspy J D, Pomeroy J M, Reader J, Feldman U and Holland G E 2008 *J. Phys. B* **41** 021003
[14] Kramida A E and Shirai T 2009 *At. Data Nucl. Data Tables* **95** 305
[15] Träbert E, Clementson J, Beiersdorfer P, Santana J A and Ishikawa Y 2010 *Phys. Rev. A* **82** 062519
[16] Kramida A 2011 *Can. J. Phys.* **89** 551
[17] Safronova U I and Safronova A S 2012 *J. Phys. B: At. Mol. Opt. Phys.* **45** 185002
[18] Kilbane D, O'ullivan G, Gillaspy J D, Ralchenko Y and Reader J 2012 *Phys. Rev.* **86** 042503
[19] Qiu M L, Zhao R F, Guo X L, Zhao Z Z, Li W X, Du S Y, Xiao J, Yao K, Chen C Y, Hutton R and Zou Y M 2014 *J. Phys. B: At., Mol. Opt. Phys.* **47** 175002
[20] Zhao R, Grumer J, Li W, Xiao J, Brage T, Huldt S, Hutton R and Zou Y 2014 *J. Phys. B: At., Mol. Opt. Phys.* **47** 185004
[21] Qiu M L, Li W X, Zhao Z Z, Yang Y, Xiao J, Brage T, Hutton R and Zou Y 2015 *J. Phys. B: At., Mol. Opt. Phys.* **48** 144029
[22] Zhao Z Z, Qiu M L, Zhao R F, Li W X, Guo X L, Xiao J, Chen C Y, Zou Y M and Hutton R 2015 *J. Phys. B: At., Mol. Opt. Phys.* **48** 115004
[23] Artemyev A N, Shabaev V M, Tupitsyn I I, Plunien G and Yerokhin V A 2007 *Phys. Rev. Lett.* **98** 173004
[24] Ralchenko Y, Draganić I N, Osin D, Gillaspy J D and Reader 2011 *Phys. Rev. A* **83** 032517
[25] Osin D, Gillaspy J, Reader J and Ralchenko Y 2012 *Eur. Phys. J. D* **66** 286
[26] Gu M F 2003 *Astrophys. J.* **582** 1241
[27] Gu M F 2008 *Can. J. Phys.* **86** 675
[28] Quinet P 2011 *J. Phys. B: At. Mol. Opt. Phys.* **44** 195007
[29] http://www.am.qub.ac.uk/darc/
[30] Fournier K B 1998 *At. Data Nucl. Data Tables* **68** 1
[31] Klapisch M 1971 *Comput. Phys. Commun.* **2** 239
[32] Fischer C F and Gaigalas G 2012 *Phys. Rev. A* **85** 042501
[33] Guo X L, Huang M, Yan J, Li S, Si R, Li C Y, Chen C Y, Wang Y S and Zou Y M 2015 *J. Phys. B: At. Mol. Opt. Phys* **48** 144020
[34] Lindgren I 1974 *J. Phys. B: At. Mol. Opt. Phys.* **7** 2441

[35] Jönsson P, Gaigalas G, Bieroń J, Fischer C F and Grant I 2013 *Comput. Phys. Commun.* **184** 2197
[36] Jönsson P, He X, Fischer C F and Grant I 2007 *Comput. Phys. Comm.* **177** 597
[37] Fei Z, Zhao R, Shi Z, Xiao J, Qiu M, Grumer J, Andersson M, Brage T, Hutton R and Zou Y 2012 *Phys. Rev. A* **86** 062501
[38] Brenner G, López-Urrutia J R C, Harman Z, Mokler P H and Ullrich J 2007 *Phys. Rev. A* **75** 032504
[39] Hao L H, Jiang G and Hou H J 2010 *Phys. Rev. A* **81** 022502
[40] Grant I P, McKenzie B J, Norrington P H, Mayers D F and Pyper N C 1980 *Comput. Phys. Commun.* **21** 207
[41] Grant I P 2007 *Relativistic Quantum Theory of Atoms and Molecules* (New York: Springer) p. 13
[42] Dyall K 1989 *Comput. Phys. Commun.* **55** 425
[43] McKenzie B J, Grant I P and Norrington P H 1980 *Comput. Phys. Commun* **21** 233
[44] Ekman J, Jönsson P, Gustafsson S, Hartman H, Gaigalas G, Godefroid M R and Fischer C F 2014 *Astron. Astrophys.* **564** 24
[45] Mohr P J 1982 *Phys. Rev. A* **26** 2338
[46] Olsen J, Roos B O, Jøgensen P and Jensen H J A 1988 *The Journal of Chemical Physics* **89** 2185
[47] Brage T and Fischer C F 1993 *Phys. Scr.* **47** 18
[48] Ding X B, Koike F, Murakami I, Kato D, Sakaue H A, Dong C Z, Nakamura NKA and Sakoda J 2011 *J. Phys. B: At. Mol. Opt. Phys.* **44** 145004